Electronic Supplementary Information (ESI) for Journal of Materials Chemistry A

Supporting Information for

WO_3 Nanolayer Coated 3D-Graphene/Sulfur Composites for High Performance Lithium/Sulfur Batteries

Sinho Choi[a†], Dong Han Seo[b†*], Mohammad Rejaul Kaiser[b†], Chunmei Zhang[c], Timothy van der laan[b,c], Zhao Jun Han[b], Avi Bendavid[b], Xin Guo[a], Samuel Yick[b], Adrian T Murdock[b], Dawei Su[a], Bo Ram Lee[d], Aijun Du[c], Shi Xue Dou[e], and Guoxiu Wang[a*]

[a]Centre for Clean Energy Technology, Faculty of Science, University of Technology Sydney, Sydney, NSW 2007, Australia.

[b]CSIRO Manufacturing, P.O. Box 218, 36 Bradfield Road, Lindfield, NSW 2070, Australia.

[c]Institute for Future Environments and Institute for Health and Biomedical Innovation, School of Chemistry, Physics, and Mechanical Engineering, Queensland University of Technology,

Brisbane, QLD 4000, Australia.

[d]Department of Physics, Pukyong National University, 45 Yongso-ro, Nam-Gu, Busan 48513, Republic of Korea.

[e]Institute for Superconducting and Electronic Materials, University of Wollongong, Wollongong, NSW 2522, Australia.

[f]KIER-UNIST Advanced Center for Energy, Korea Institute of Energy Research (KIER), Ulsan 44919, South Korea.

This PDF file includes:

Figs. S1 to S14

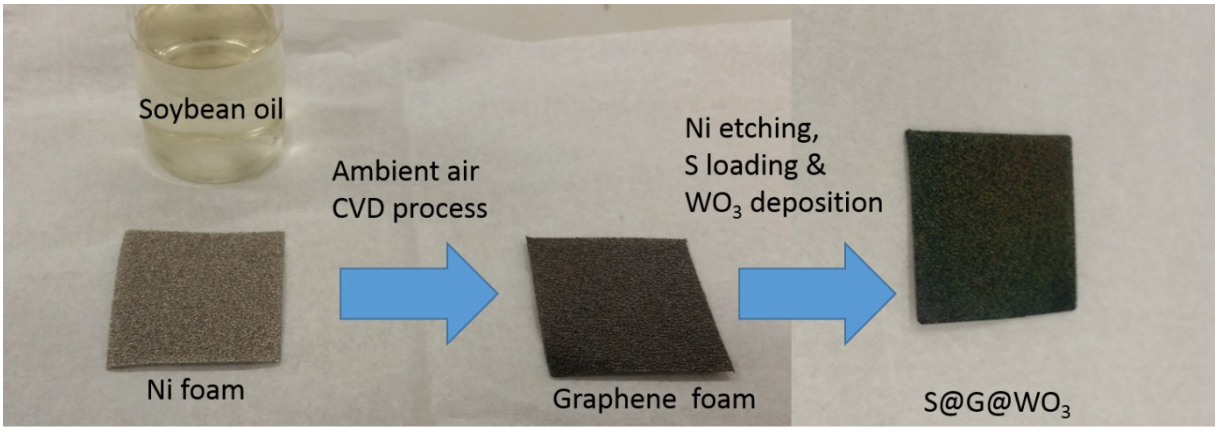

Figure S1. Photographs of the different steps of synthesizing the S@G@WO_3 composite with soybean oil as the precursor and Ni foam as the template.

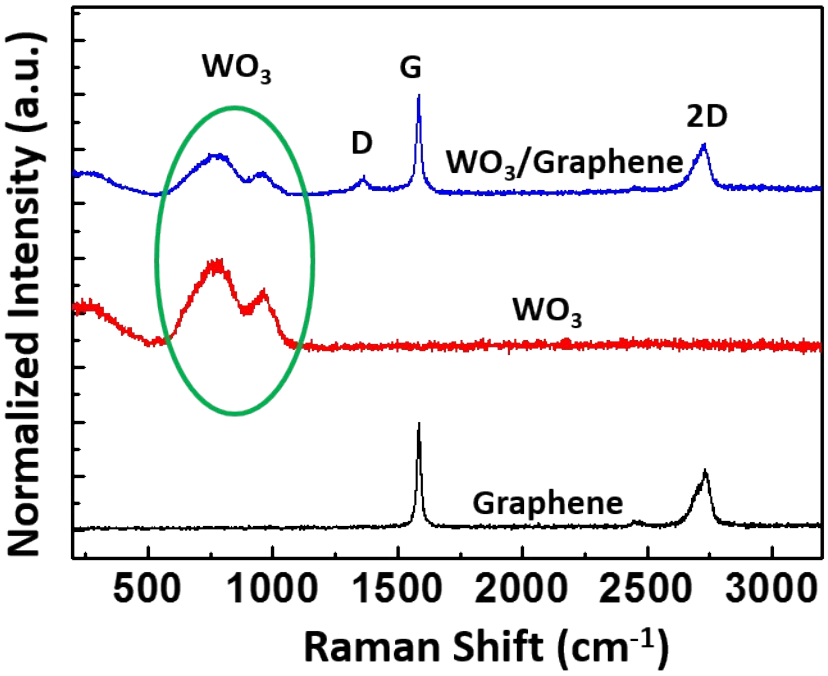

Figure S2. Raman spectra of graphene, WO_3 and WO_3/Graphene composite.

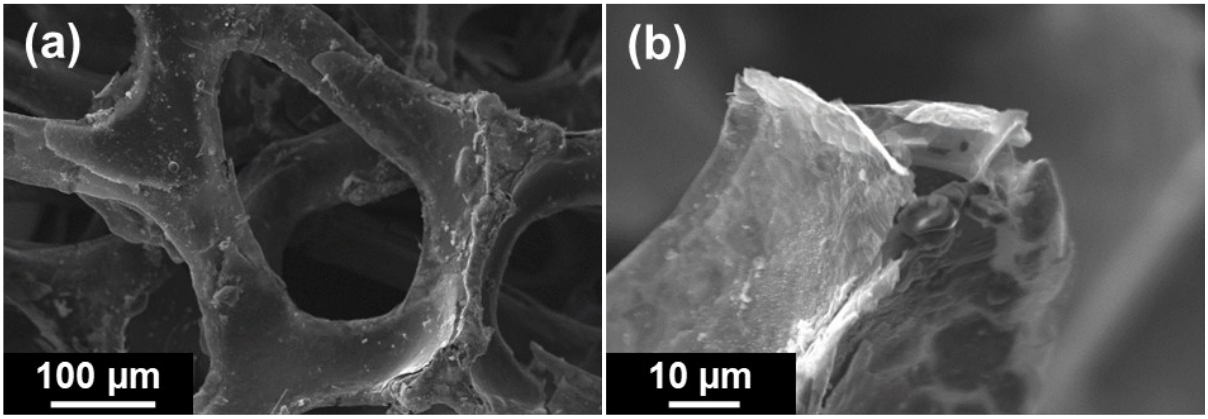

Figure S3. SEM image of 3D graphene (a) before and (b) after Ni foam is etched.

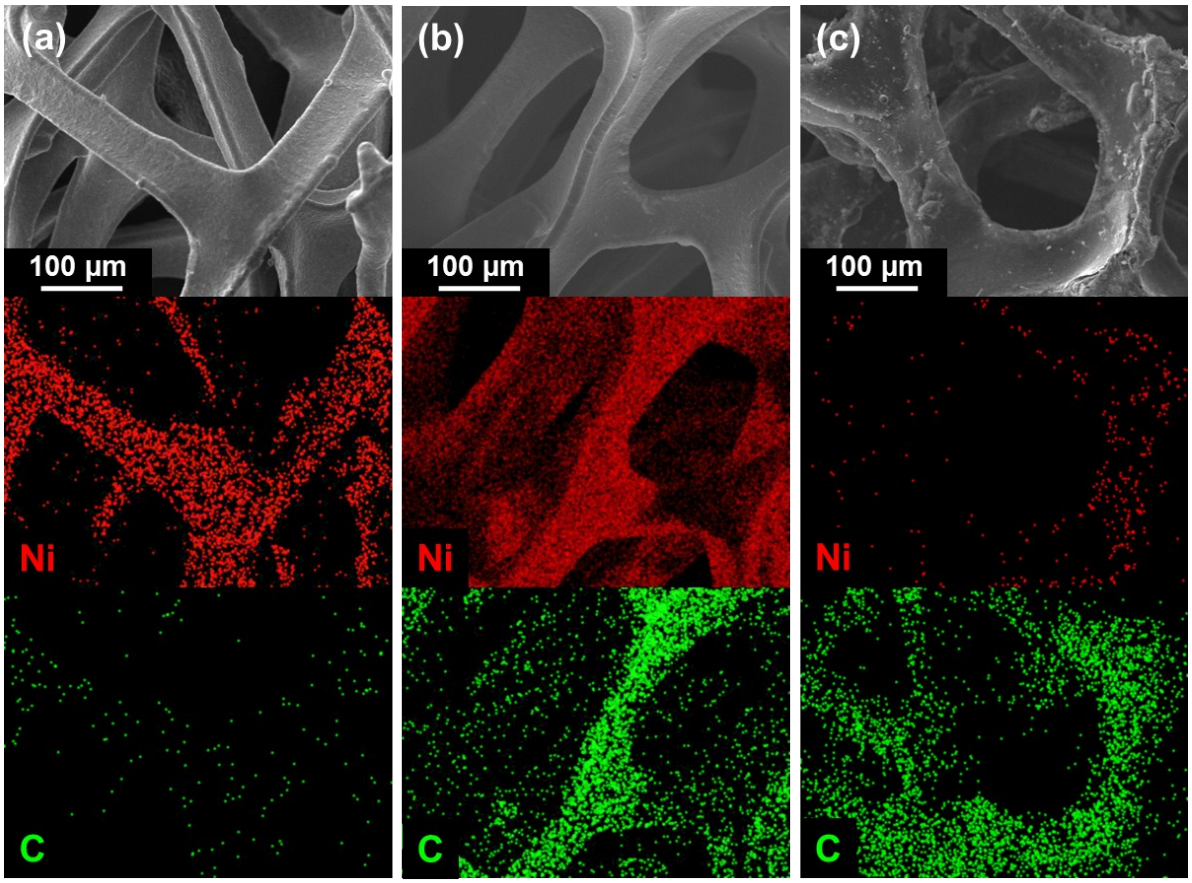

Figure S4. EDS analysis of column-a) Ni foam template, column-b) graphene-coated Ni foam (before HCl etch) and column-c) 3D graphene foam (after HCl etch).

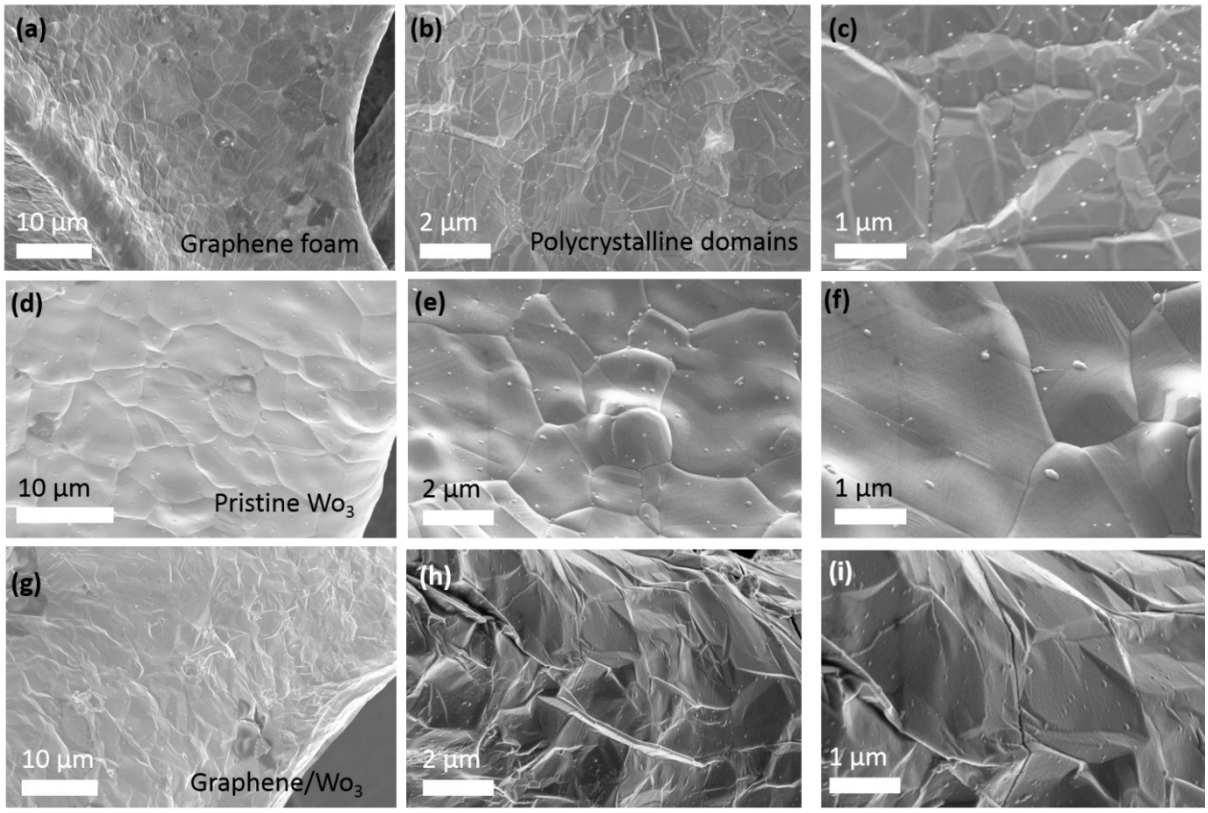

Figure S5. SEM images of (a-c) graphene-coated Ni Foam, (d-f) WO_3-coated Ni Foam and (g-i) WO_3/graphene-coated Ni Foam at different magnifications.

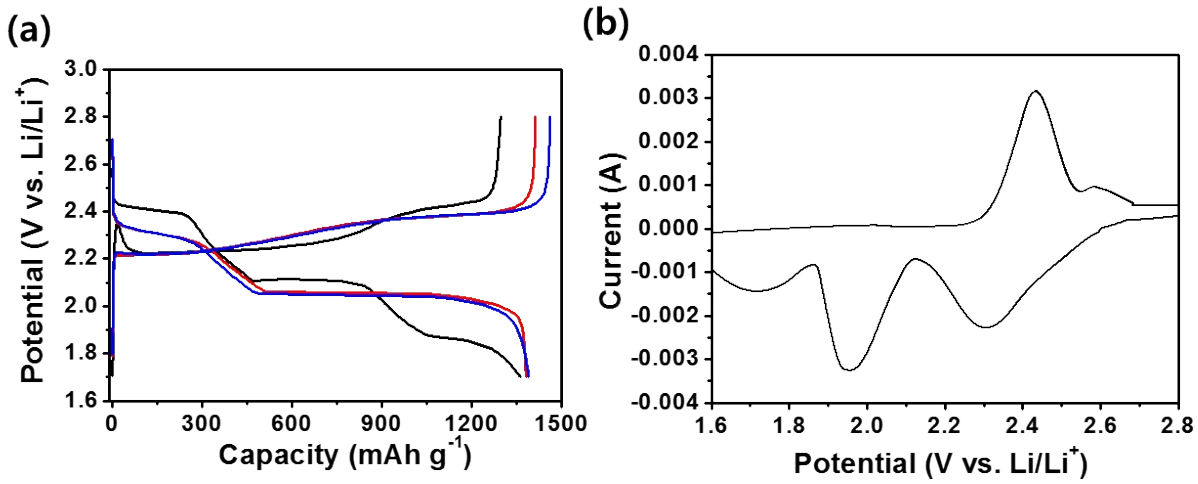

Figure S6. (a) Charge discharge curves at 0.8 A/g of S@G@WO_3 electrode at 1st (black), 100th (red), 500th cycles (blue) and (b) CV curve of S@G@WO_3 electrode at 0.75 mV/s.

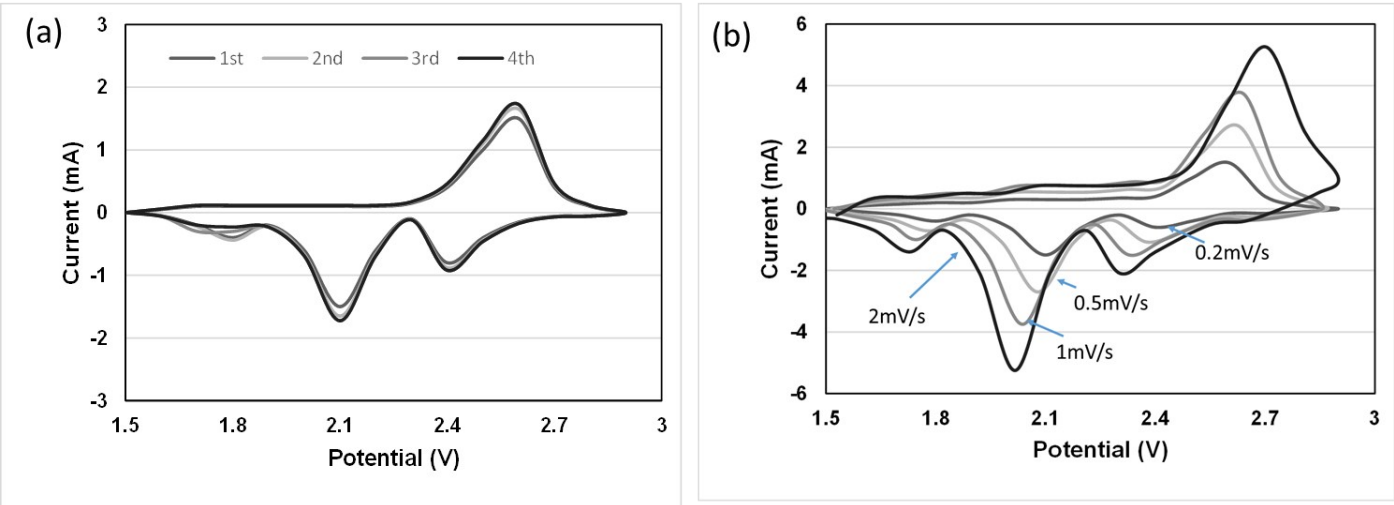

Figure S7.(a) CV curves of S@G@WO_3 electrode at constant scan rate of 0.2mV/s, one can observe disappearance of 3rd peak during the discharging process after 3rd cycles (b) CV curves of S@G@WO_3 electrode at different scan rates (0.2mV/s ~ 2mV/s).

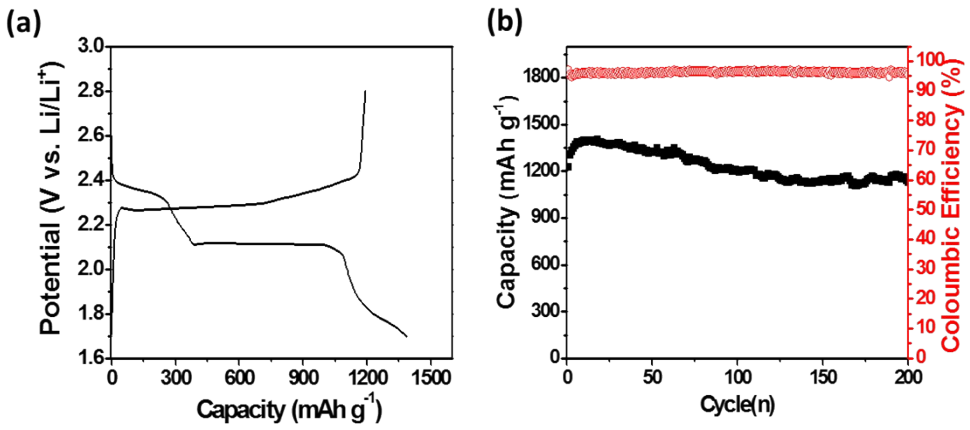

Figure S8. (a) Charge discharge curve (1st cycle) at 1.6 A/g of S@G@WO_3 electrode and (b) cycling performance (capacity and Coulombic efficiency) at 1.6 A/g (~ 1C).

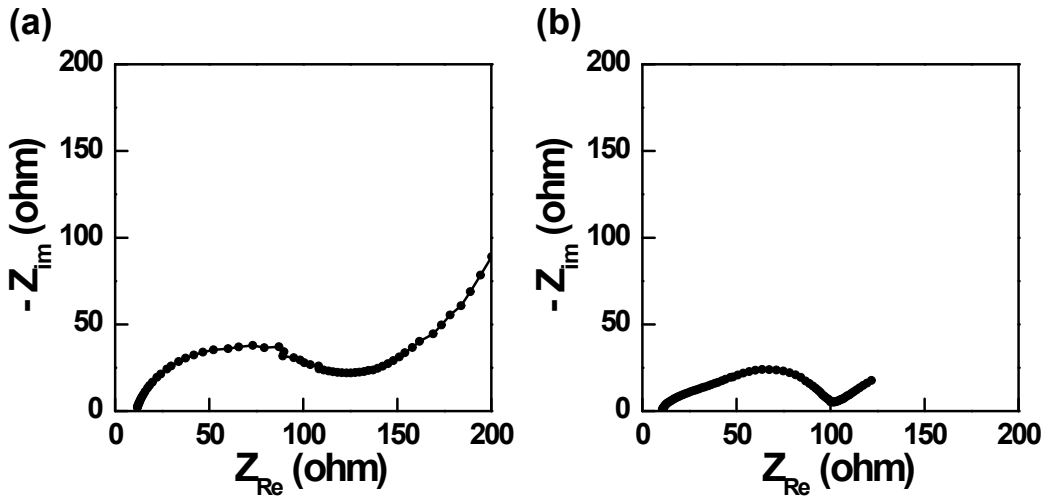

Figure S9. Nyquist plots of the (a) S@G and (b) S@G@WO_3 electrode.

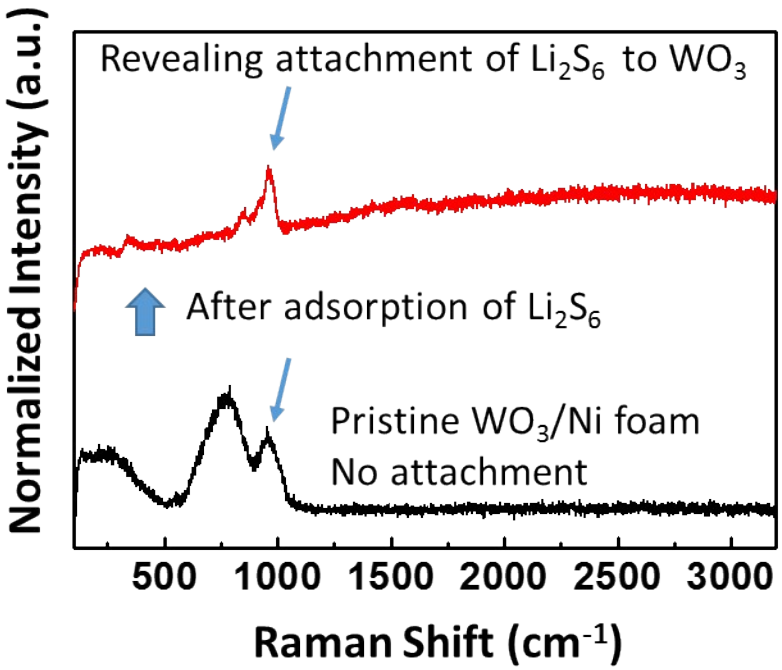

Figure S10. Raman spectra of the graphene-free WO_3/Ni cathode before and after adsorption of Li_2S_6.

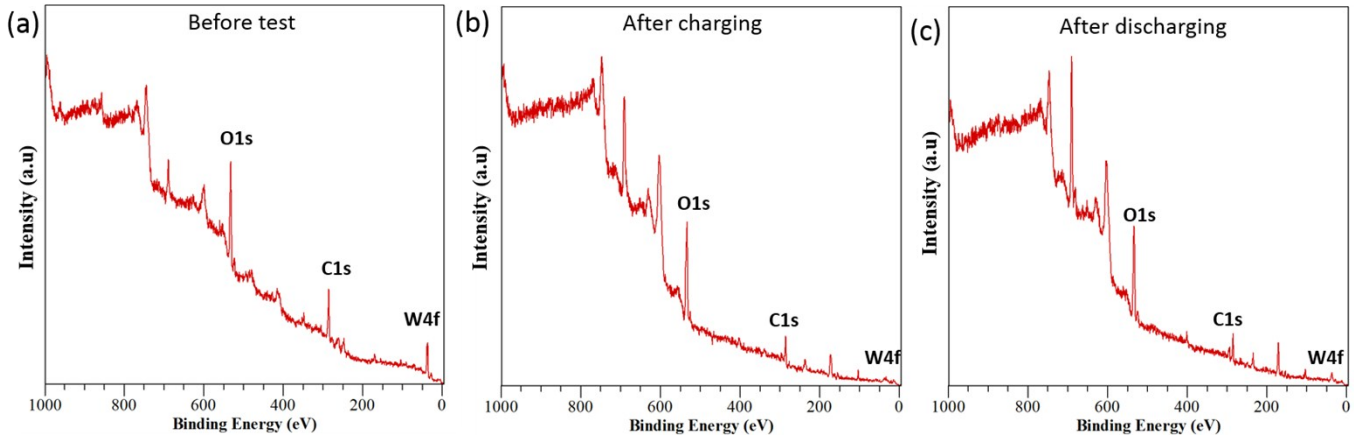

Figure S11. XPS survey spectra of S@G@WO_3 electrode (a) before, (b) after charging, (c) after discharging cycles.

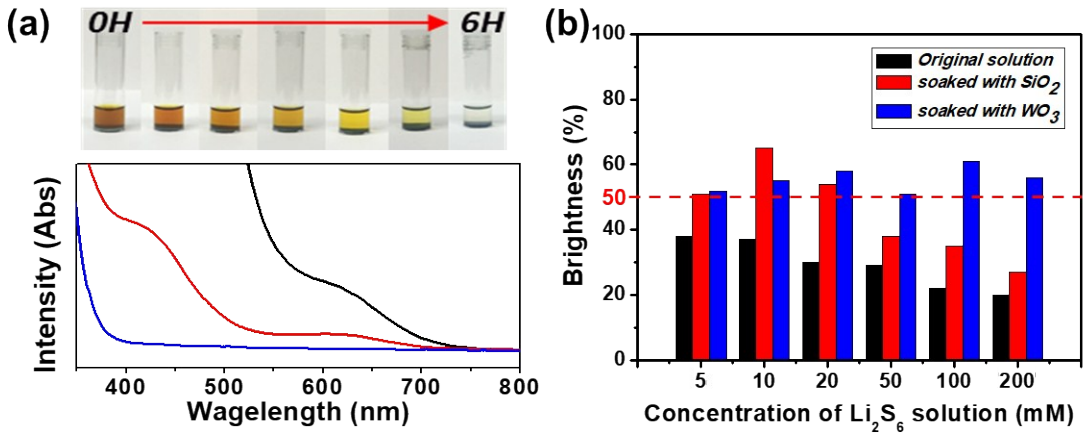

Figure S12. (a) The top photos show a time series (0 hours to 6 hours) for the absorption of Li_2S_6 by WO_3, the bottom UV-Vis absorption spectra shows the capability of Li_2S_6 polysulfide absorption by WO_3 (blue line) and SiO_2 (red line) and (b) the bar chart shows the comparison of absorption of Li_2S_6 for different concentrations by WO_3 and SiO_2.

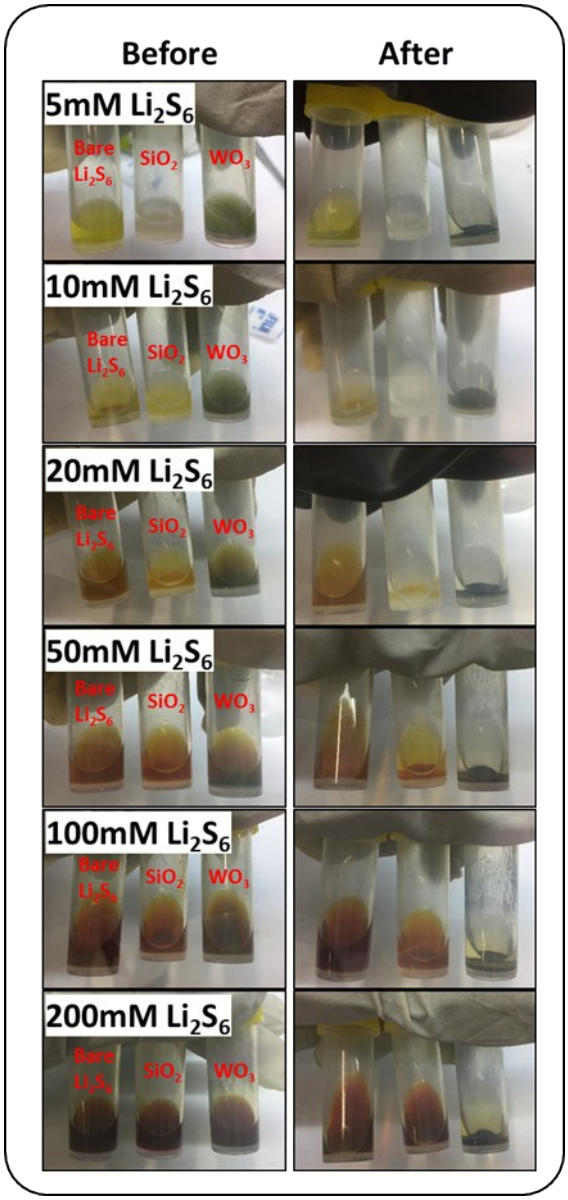

Figure S13. Photos and visual observations of Li_2S_6 polysulfide absorption by SiO_2 and WO_3 at different concentrations.

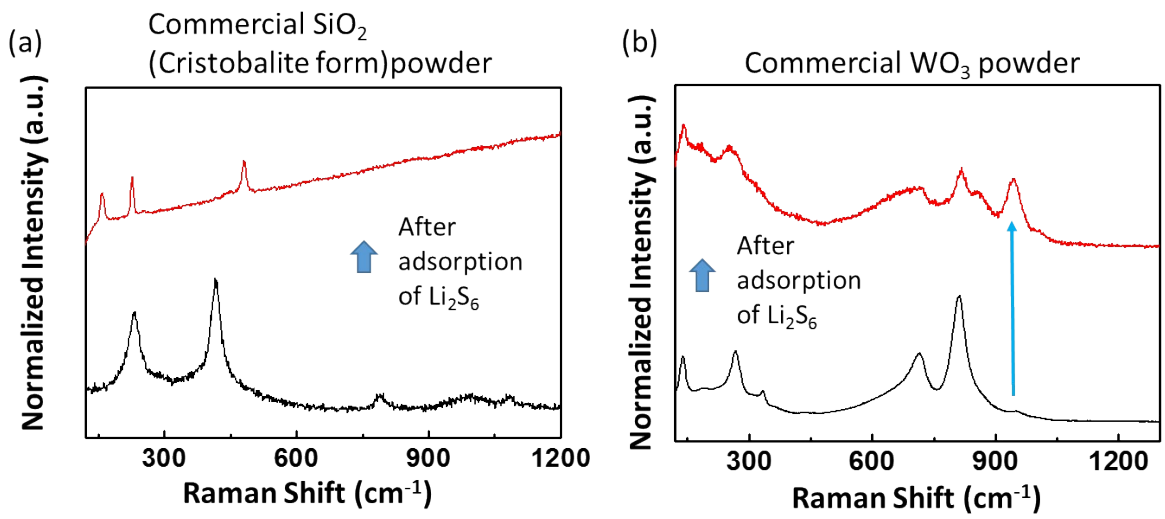

Figure S14. Raman analyses of the commercial (a) SiO_2 and (b) WO_3 powders before and after adsorption of Li_2S_6.